Turbulence in Active Matters

Zhiru Liu*
Term Essay for PHYS 569†
University of Illinois at Urbana-Champaign

Abstract

The presence of active particles in fluid often results in complex collective patterns and dynamics. In this essay, we focus on a particular non-equilibrium phase that resembles turbulence in classical fluid dynamics. We review both the experimental setups and the candidates of modeling this phenomenon. Power laws in the energy spectrum have been found in both experiments and simulations, but controversy exists.

*zliu106@illinois.edu
†http://guava.physics.uiuc.edu/ nigel/courses/569/

1 Introduction

Turbulence is often considered the most important unsolved problem in classical physics. Its ubiquitous presence in almost all fluid systems and the mathematical difficulties involved have driven many decades of intensive research but understandings are still insufficient.[1] The study of fluid motion, nevertheless, can be further complicated when the fluid is turned into active matter. Active matter refers to systems composed of many active agents, each of which is capable of moving on its own. Bacterial suspension, for example, is an active fluid with rich collective behaviours. Remarkably, recent studies have uncovered a turbulent phase of bacterial suspension, which is analogous to classical turbulence in many ways. In this essay, we provide a review of both experimental and theoretical results related to this "active turbulence."

2 A review of classical turbulence

Before introducing active turbulence, it is beneficial to briefly review the key concepts in classical turbulence. We will only focus on the phenomena that have analogous counterparts in active turbulence.

2.1 The Navier-Stokes equation

It is believed that all the wonderful physics of turbulence can be captured by the Navier-Stokes equation:

$$\partial_t \mathbf{v} + \mathbf{v} \cdot \nabla \mathbf{v} = -\nabla p + \nu \nabla^2 \mathbf{v} \tag{1}$$

$$\nabla \cdot \mathbf{v} = 0 \tag{2}$$

where the ν term describes viscous effect, ∇p describes the force due to pressure, the nonlinear term describes convection and eq.2 is the usual continuity equation under the assumption of incompressible fluid.

2.2 Reynolds number

An important control parameter for experiments is the Reynolds number:

$$R = \frac{LV}{\nu} \tag{3}$$

where L and V are the characteristic length scale and flow velocity of the system, and ν is the kinematic viscosity. Turbulent effect becomes significant when $R \sim 1000$.

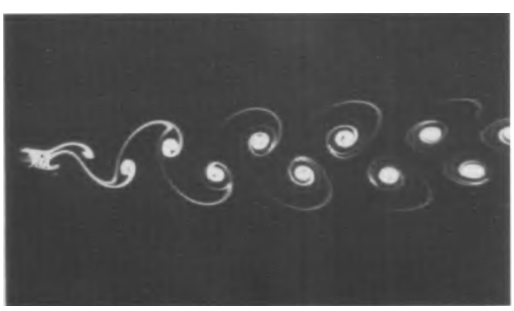

(a) Karman vortex street behind a circular cylinder at $R = 105$.

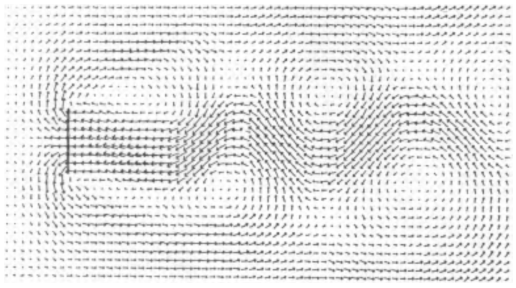

(b) Lattice gas simulation of a two-dimensional Karman vortex street behind a flat plate.

Figure 1: Some visualization of eddies.[1]

2.3 Eddies and cascades

Eddies are often used interchangeably with vortices, and both do not have very precise definitions. Roughly speaking, an eddy refers to a swirling fluid motion with a characteristic length, velocity and time scale. The visualizations of eddies in fig.1 provide some intuitive understandings.

In the turbulent flow, many eddies of different scales exist and energy is transported between them. As first observed by Richardson, big eddies break up into small eddies, and small eddies break up into even smaller ones. In this way, kinetic energy is transported from the large scales of the motion all the way down to the smallest scale of motion, where viscosity affect the dynamics and dissipates the energy. This process can be quantified as we will shortly see.

2.4 Quantitative results

Two functions are usually used to describe the statistics of experimental data in turbulence, namely the structure functions and the energy spectrum. Let us define several quantities. The longitudinal velocity increment is defined

as

$$\delta v_{\parallel}(\mathbf{r},\mathbf{l}) = (\mathbf{v}(\mathbf{r}+\mathbf{l}) - \mathbf{v}(\mathbf{r})) \cdot \frac{\mathbf{l}}{l} \tag{4}$$

and the n-th structural function is

$$S_n(\mathbf{l}) = \langle [\delta v_{\parallel}(\mathbf{r},\mathbf{l})]^n \rangle \tag{5}$$

where the average is taken over space.

The energy spectrum is formally defined as

$$\frac{1}{2}\langle \mathbf{v}^2 \rangle = \int_0^\infty E(k)dk \tag{6}$$

and the energy spectrum can be written as

$$E_d(k) = \frac{k^{d-1}}{C_d} \int d^d R e^{-i\mathbf{k}\cdot\mathbf{R}} \langle \mathbf{v}(\mathbf{r}) \cdot \mathbf{v}(\mathbf{r}+\mathbf{R}) \rangle \tag{7}$$

where d is dimension, $C_2 = 2\pi$ and $C_3 = 4\pi$.

Komogorov's famous 1941 theory predicts that $E(k) \sim k^{-5/3}$[1], and this power law is widely accepted by experimental tests. For example,fig.2a is a typical experimental demonstration of this power law. The range that the power law holds is called the "inertial range." The interpretation of this kind of spectra is that the energy is injected at the large length scale, the left end of the inertial range, and then propagated through the cascade to smaller scales, until eventually dissipated at the right end of the inertial range. However, dimension plays an important role in turbulence. In two dimension, there might be an inverse cascade with a different power law[2], like in 2b.

3 Active turbulence

3.1 Experimental methods

We now turn to the phenomena of active turbulence.

Droplets of bacteria suspension The existence of a turbulent phase in bacterial suspensions was perhaps earliest reported by Dombrowski et al., who pointed out that the bacterial vortices seen in fig.3 are similar to a

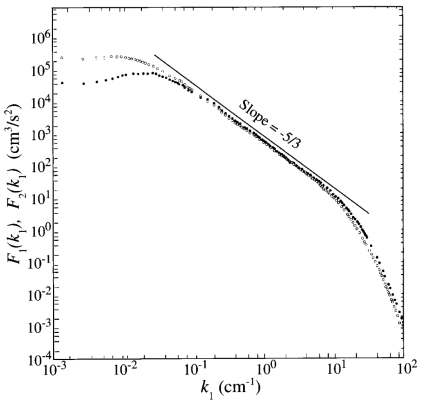

(a) Experimental data of 3D turbulence that obey a clean five-third law[1].

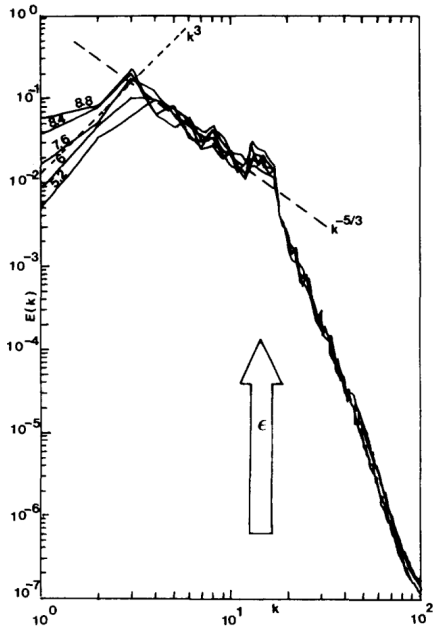

(b) Experimental data of 2D turbulence with two cascades.[2]

Figure 2: Energy cascades in classical turbulence.

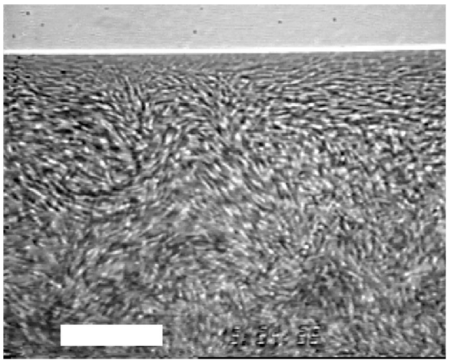

(a) Turbulent motion of bacteria. The scale bar is $35\mu m$.

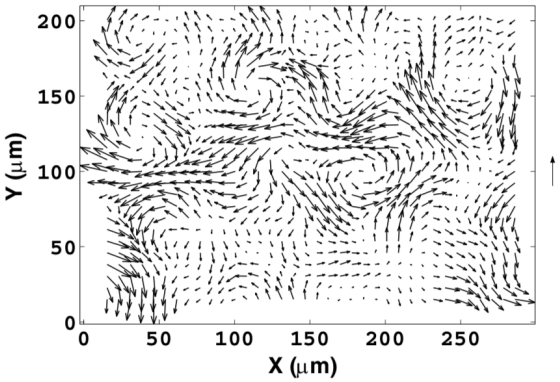

(b) The velocity field of bacterial flow. The arrow denotes speed of $35\mu m/s$.

Figure 3: Turbulent motion in a bacterial droplet[3].

von Karman vortex street[3]. The velocity field was obtained by particle-imaging-velocimetry (PIV, Dantec), which means the bacteria also serve as the marker in the fluid. However, the sessile or pendant suspension drops they used were not controlled in concentration, and whether bacteria motion can accurately reflect fluid motion remains in question.

Bacteria suspension in chambers In the droplets experiments, chemotaxis plays an important role in bacterial dynamics. To reduce this effect and further simplify the study, experiments have been done in closed chambers[4][5]. Two kind of geometries were used: a quasi-2D and a 3D microfluid chamber. The vertical height of the quasi-2D chamber is less than or equal to the body length of *B. subtilis*. It is noteworthy that such a geometry is different from a 2D free standing film. In 3D fluid, the far-field flow created by a *B. subtilis* decays as $1/r^2$. However, when the swimmer is swimming parallel to a nearby solid surface, the parallel flow component decays as $1/r^4$. And the flow decays exponentially when the swimmer is confined between two parallel solid surfaces. Therefore, in the quasi-2D chamber, the hydrodynamic interactions (i.e. interactions via flows) are less important than other geometries and the model can be simplified. Lastly, the bacterial suspension used in the experiment was prepared at high filling fraction ($\geq 50\%$).

Swarming sperm In addition to swimming bacteria, swarming sperms were also found to exhibit self-sustained turbulent motion. Ram semen was used for its naturally high concentration($\geq 50\%$). Similar to the bacterial suspension case, the samples were confined in near two dimensional chambers with vertical heights around hundreds micrometers. Fig.4 demonstrates the turbulent motion of swarming sperms. We see that all three cases mentioned thus far produce qualitatively similar patterns, and they all differ from classical turbulence because the Reynolds numbers are much lower.

PIV vs. PTV As mentioned earlier, the flow of the solvent medium might be different from the flow of the active swimmers. In particle image velocity (PIV) algorithm, each frame is devided into small windows and the most probable displacement is estimated by comparing two successive frames[6]. In this sense, the active swimmers, who contribute to the pattern of each window, are themselves markers of the flow. On the other hand, particle tracking velocity (PTV) employs fluorescent microparticles that move with

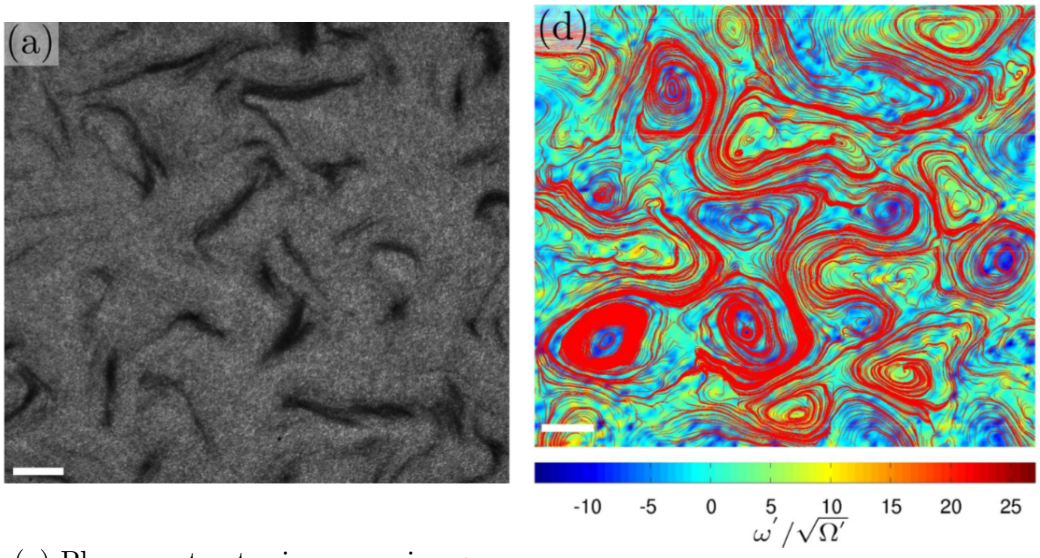

(a) Phase-contrast microscope images.

(b) The vorticity field.

Figure 4: Turbulent motion of fresh semen placed between two glass plates separated by $100\mu m$. The scales bars are $200\mu m$[6].

the medium to estimate the flow of the medium[6]. The hypothesis that PIV can accurately describe the fluid motion was tested in both the bacterial suspension experiment and the swarming sperm experiment[5][6]. The researchers concluded that the velocity field measured from PIV is very close to the true values measured by PTV.

3.2 Models of active turbulence

Another way to study active turbulence is through simulation, which requires an effective model that captures the physics. We will focus on two models proposed by Wensink et al., which were proved effective in describing the collective motion of active agents[4].

Microscopic model The microscopic model is a minimalistic two-dimensional model that was proposed to simply the interactions inside a bacterial suspension. In this self-propulsion rod model (SPR model), bacteria are modeled as rigid rods moving under a constant self-propulsion, and they interact with each other through a Yukawa potential ($\sim exp(r/\lambda)/r$, where r is distance

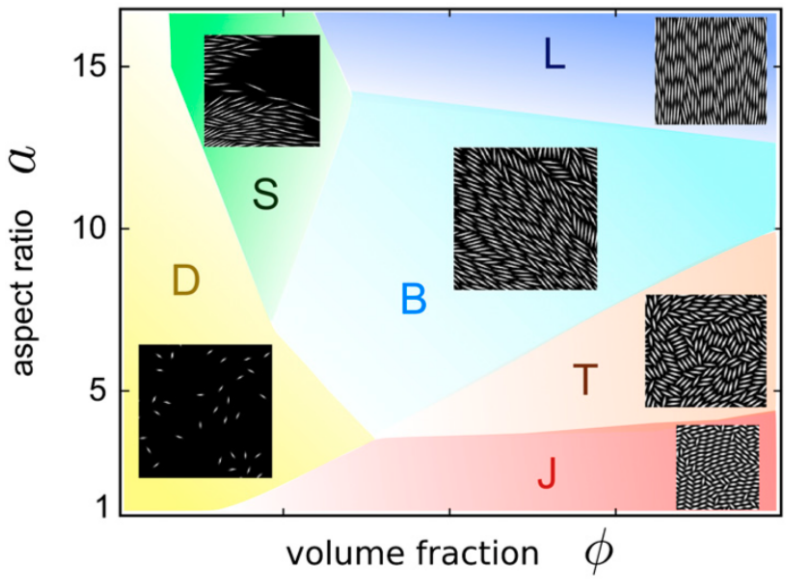

Figure 5: The phase diagram of the 2D SPR model.[4] D for dilute, S for swarming, B for bionematic, J for jamming, L for laning and T for turbulent.

and λ is the screening length) to ensure the screening effect in dense suspensions.

With this microscopic model, the aspect ratio and the filling fraction of agents can be easily changed and thus a phase diagram in those two parameters can be obtained. The resulting phase diagram is shown in fig.5. We can see that the turbulent phase requires a high filling fraction. The range of the aspect ratio that admits turbulence, on the other hand, covers typical bacteria like *E. coli* and *B. subtilis*.

Continuum model The continuum model was an extension to the Navier-Stokes equation with extra terms inspired by Toner-Tu equation and Swift-Hohenberg equation.[4] Since the active fluid in turbulent phase has a high filling fraction, the density fluctuation is often negligible, in contrast to other scenarios such as flocking. As a result, incompressibility was assumed, $\nabla \cdot \mathbf{v} = 0$. Then, the proposed model is

$$(\partial_t + \lambda_0 \mathbf{v} \cdot \nabla)\mathbf{v} = -\nabla p + \lambda_1 \nabla \mathbf{v}^2 - (\alpha + \beta|\mathbf{v}|^2)\mathbf{v} + \Gamma_0 \nabla^2 \mathbf{v} - \Gamma_2 (\nabla^2)^2 \mathbf{v} \quad (8)$$

In addition to the usual Navier-Stokes terms, the first and third order terms in $\mathbf{v}$ correspond to a force caused by a Landau-type quartic potential $U = \alpha/2|\mathbf{v}|^2 + \beta/4|\mathbf{v}|^4$, and the fourth order derivative term plays a similar role as quartic potential in Fourier space[4].

Validation of the models To see that the both the SPR model and the continuum model qualitatively match the real dynamics, the researchers compared the simulations with the previously mentioned quasi-2D experiment. The vorticity field, defined as

$$\omega(x, y) = \partial_x v_y(x, y) - \partial_y v_x(x, y) \tag{9}$$

can provide a clear visualization of the complicated vortices. As we can see, fig.6 B,C and D have qualitatively same patterns, thus justifying the validity of the model. Further quantitative justifications will be presented in the next section.

Other variants Some other variants of eq.1 are also used in the study of active turbulence. For example, in [7], the authors introduced a sixth order derivative term through a phenomenological stress tensor

$$\sigma = (\Gamma_0 - \Gamma_2\nabla^2 + \Gamma_4\nabla^4)[\nabla\mathbf{v} + (\nabla\mathbf{v})^{\mathbf{T}}] \tag{10}$$

and

$$(\partial_t + \mathbf{v}\cdot\nabla)\mathbf{v} = -\nabla p + \nabla\cdot\sigma \tag{11}$$

Another example is a model termed "active nematdynamics" in [8], where the velocity field is coupled with a alignment tensor.

3.3 Quantitative results

We now present various quantitative results from experiments as well as direct simulation of the models introduced.

Structure functions The structure functions of bacterial suspensions were calculated in both experimental and numerical data. (Fig.7) This comparison further demonstrate the validity of 2D SPR model and continuum model. Notice that dimensional effect is significant in all structure functions of order

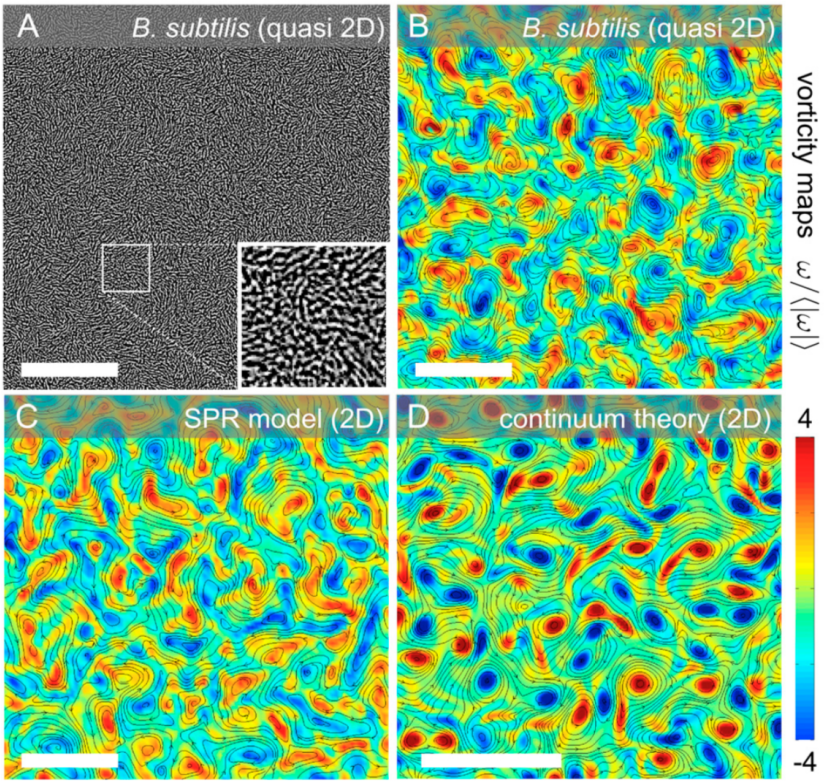

Figure 6: A comparison between experiments and simulations of two models for bacterial suspension.[4]

larger than one. Both minimal models produce structure functions reasonably close to those of experiments. However, the microscopic model appears to be less accurate than the phenomenological continuum model, possibly because of the oversimplification of the interactions.

Energy spectra and power laws A diverse yet confusing collection of power laws were found in the experiments and simulations. The results are summarized in fig.8. Each paper claimed to find a different form of energy cascade and some of them are contradictory to others, even in the same dimensions. For example, while the active nematdynamics simulation (8c) shows that the exponent does not depend on model parameters, the continuum model simulation (8d) shows that the exponent does depend on the parameters. In fact, it was found in [9] that the exponent of the power

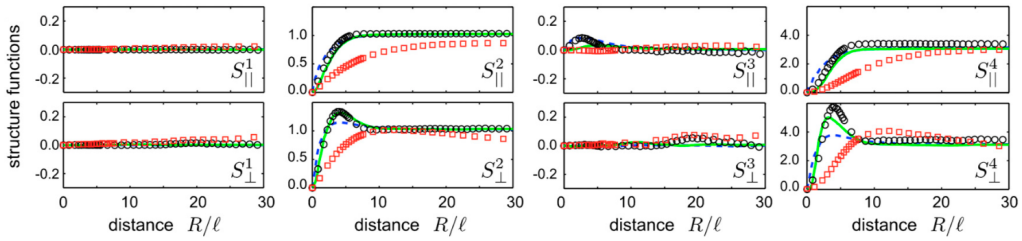

Figure 7: Different order of structure functions[4]. The definition for longitudinal ones can be found in 5. Similar for transverse ones. Green curves are the continuum model, blue dash lines are the SPR model, black circles are the quasi-2D experiments and red squares are the 3D experiments.

law depends nearly linearly on the self-propulsion strength α.

Also, although both 8a and 8d use the same 2D continuum model, 8d identifies the second power law in 8a as exponential decay. More precisely, in the paper[9], a semianalytical result was found

$$E_k = \tilde{E}_0 k^\delta exp(-\frac{\Gamma_0}{\lambda_0 \omega_c} k^2) \tag{12}$$

Since both curves bend downward at large k, the above result is still not accurate enough.

4 Conclusion

Although the existing models of active turbulence succeeded in reproducing turbulent patterns at low Reynolds numbers as well as some statistics of the data, the field seems to reach no consensus yet. Each of the additional nonlinearity and high derivatives make the already hard Navier-Stokes equation even more intimidating to approach analytically. The various power laws, unlike classical turbulence, depends not only on dimension but also on specific parameters of the active swimmer. More experiments are needed to clarify whether the claimed power laws regimes are as robust as those in classical turbulence. Nevertheless, it is intriguing that the dynamics is changed completely with a few more extra terms. The Landau type arguments and the emergence of complex phenomena from simple models connect with the content of the course, and the author is excited to learn more about biological emergence after these readings.

References

[1] Uriel Frisch. *Turbulence: The Legacy of A. N. Kolmogorov*. Cambridge University Press, 1996.

[2] U. Frisch and P.-L. Sulem. Numerical simulation of the inverse cascade in two-dimensional turbulence. *Physics of Fluids*, 27(8):1921, 1984.

[3] Christopher Dombrowski, Luis Cisneros, Sunita Chatkaew, Raymond E. Goldstein, and John O. Kessler. Self-concentration and large-scale coherence in bacterial dynamics. *Physical Review Letters*, 93(9), aug 2004.

[4] H. H. Wensink, J. Dunkel, S. Heidenreich, K. Drescher, R. E. Goldstein, H. Lowen, and J. M. Yeomans. Meso-scale turbulence in living fluids. *Proceedings of the National Academy of Sciences*, 109(36):14308–14313, aug 2012.

[5] Jörn Dunkel, Sebastian Heidenreich, Knut Drescher, Henricus H. Wensink, Markus Bär, and Raymond E. Goldstein. Fluid dynamics of bacterial turbulence. *Physical Review Letters*, 110(22), may 2013.

[6] Adama Creppy, Olivier Praud, Xavier Druart, Philippa L. Kohnke, and Franck Plouraboué. Turbulence of swarming sperm. *Physical Review E*, 92(3), sep 2015.

[7] Jonasz Słomka and Jörn Dunkel. Spontaneous mirror-symmetry breaking induces inverse energy cascade in 3d active fluids. *Proceedings of the National Academy of Sciences*, 114(9):2119–2124, feb 2017.

[8] Luca Giomi. Geometry and topology of turbulence in active nematics. *Physical Review X*, 5(3), jul 2015.

[9] Vasil Bratanov, Frank Jenko, and Erwin Frey. New class of turbulence in active fluids. *Proceedings of the National Academy of Sciences*, 112(49):15048–15053, nov 2015.

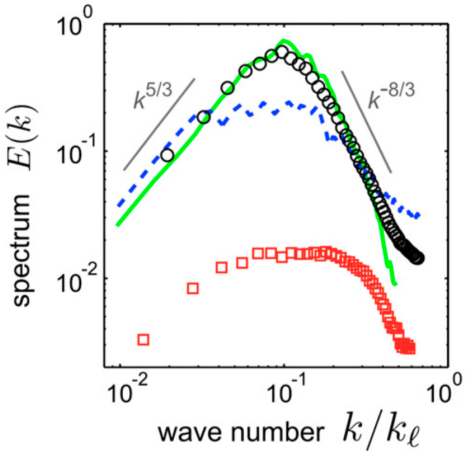

(a) Energy spectrum of bacterial suspension in quasi-2D and 3D chambers. The circles are quasi-2D, and red squares 3D. The green curve is the 2D continuum model and blue dash curve is the 2D microscopic model.[4]

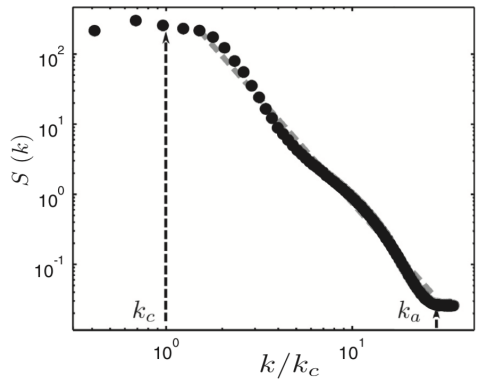

(b) Energy spectrum of swarming sperm in quasi-2D chamber[6]. The regime $[k_c, k_a]$ is claimed to follow a k^{-3} power law.

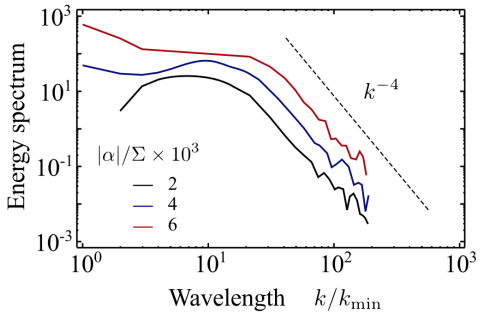

(c) The energy spectrum of simulations of the active nematdynamics model[8]. Different curves correspond to different activity values, which can be roughly understood as the magnitudes of the self-propulsion force.

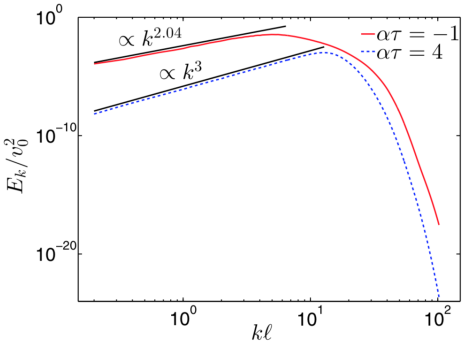

(d) The energy spectrum of simulations of the 2D continuum model[9]. Different curves correspond to different different intensities of energy injection. α appears in the right hand side of eq.8 and τ is a time scale defined with other parameters.

Figure 8: Comparison between power laws.